Interferon-induced lysosomal membrane permeabilization causes cDC1-deserts in tumors.

[1,2]E. Aerakis, [1]A. Chatzigeorgiou, [1]D. Kerdidani, [1] I. Angelidis, [1]M. Matthaiakaki-Panagiotaki, [3]B. Malissen, [3]S. Henri and [1]M. Tsoumakidou*.

[1]Institute of Bioinnovation, BSRC Alexander Fleming, Vari, Greece
[2]Laboratory of Physiology, Medical School, National and Kapodistrian University of Athens, Greece
[3]Centre d'Immunologie de Marseille-Luminy, Aix Marseille Université, INSERM, CNRS, Marseille, France

*Corresponding author. Maria Tsoumakidou, Institute of Bioinnovation, BSRC "Alexander Fleming", Greece, 16672. Phone:(167)+30-210-9653310; Fax: +30-210-9653934; E-mail: tsoumakidou@fleming.gr

Abstract

The landscape of migratory conventional dendritic cells (cDCs) comprises XCR1^{+}CD11b^{-} cDC1s, XCR1^{-}CD11b^{+} cDC2s and intermediate XCR1$^{low/neg}$CD11b^{-} states. cDC1 are unique in their ability to cross-prime lymph node CD8 T cells in a CD4 T cell-dependent manner. In perturbed cancer states cDC1s become particularly scarce in tumors and tumor draining lymph nodes, which decreases T cell infiltration, immunotherapy responses and patient survival. The causes of cDC1 paucity are not fully understood and no specific therapy currently exists. Here, we find that cDC1s undergo apoptosis in tumor microenvironments. Gene expression analysis of independent murine and human RNA sequencing datasets point to a shared cDC1 lysosomal stress response state across various tumors. Modeling primary cDC1 behavior in lung tumors in vivo and ex vivo, we show that two distinct yet interconnected pathways converge to cause apoptosis of cDC1: mTOR inhibition leads to an increase in the proteolytic activity of lysosomes, while lysosomal membrane permeabilization (LMP) allows the release of proteolytic enzymes to the cytosol and apoptotic death. Pathway and regulon analysis of the cDC1 transcriptome suggest that mTOR inhibition and lysosomal stress happen downstream of type I IFNs. Accordingly, exposure of the Mutu cDC1 line to type I IFNs inhibits mTOR, stresses lysosomes and triggers LMP and death. Further supporting this finding, in mixed bone-marrow chimeras IFNRA deletion rescues primary cDC1s from mTOR inhibition, lysosomal stress, LMP and death. We have therefore elucidated IFN-induced lysosomal death as a key mechanism of cDC1s paucity in tumors that should be prevented to increase tumor immunity through reinvigoration of the cDC1 pool.

Introduction

"All things excellent are as difficult as they are rare", Baruch Spinoza.

Immune cell co-evolution led to the emergence of diverse antigen presenting cell (APC) states and their spatiotemporal organization in lymphoid and non-lymphoid tissues [1]. In a hypothetical snapshot of the antigen presenting cell pool of an organism the vast majority would be non-professional "accessory" APCs that shape and sustain rather than prime adaptive immune responses [2]. Rare subsets of professional APCs, i.e. dendritic cells (DCs), have been assigned the exclusive task of transferring antigens from non-lymphoid tissues to lymph nodes (LNs) for naive T cell priming [3-7]. $XCR1^{+}CD11b^{-}$ conventional DCs type 1 (cDCs1) sequentially and in a coordinated manner with cDC2 present and cross-present exogenous antigens to CD4+ and CD8+ T cells, respectively, leading either to their priming or tolerization [8-12]. Tumor immune rejection directly depends on cancer-antigen specific T cells and as such on cDC1s [13]. Three lines of evidence strongly support this hypothesis: i) prolonged survival is observed in cancer patients with higher cDC1 infiltration [8, 14-16], ii) cDC1 ablation or their conditional editing in animal models impacts immunity and accelerates cancer progression[17, 18], iii) cancer immunotherapy responses depend on cDC1 mobilization [14, 19-22]. These observations are particularly impressive considering that cDC1s are rare in unperturbed tissues, comprising less than <0.1% of total cells and become scarce, reaching as few as <0.01% of total cells, in tumors [23, 24].

Single cell sequencing methodologies have advanced our understanding of antigen presenting cell diversity and dynamics in tumor microenvironments. Tumor cDC states align across murine and human datasets suggesting common developmental trajectories and universal responses to shared stimuli across different tumor ecosystems [25]. Due to their scarcity, which hampers experimentation, tumor cDC1s remain poorly understood. An additional bottleneck has been the discovery in lung tumors of CCR7 expressing $XCR1^{int/neg}CD11b^{-}$ cDC1/cDC2 intermediate states, termed mReg cDCs, that are characterized by a mixed mature-regulatory co-expression module [26]. mRegs seem to emerge from cDC1s and cDC2s in response to cancer antigen uptake and fail to express a clear mature-stimulatory profile, under the pressure of suppressive tumor stimuli, such as IL4. Conversely, IFNg-induced NF-kb and IRF1 drive immunostimulatory anti-tumor cDC1 states. CCR7+ DC3 and LAMP3+ cDCs, discovered in various tumors, likely refer to the mReg lung cDC state [27-29].

A few explanations have been given for the cDC1 deserts in tumors. Tumor-produced granulocyte-stimulating factor has been shown to downregulate bone marrow cDC progenitors, including, but not limited to cDC1 [30]. Decrease in NK- cell-derived XCL1 and development of a general immunosuppressive microenvironment by cancer cells may impede tumor cDC1 infiltration [14, 15, 22, 31-33]. However, XCL1 is redundant for cDC1 migration and other tumor repressed chemokines are not cDC1 specific. Adding another level of complexity, tumor-draining LNs themselves become deserted from cDC1s as cancer progresses and this has been attributed to impaired LN migration[26]. Here we show that cDC1s enter a lysosomal stress response state and succumb to cell death in tumors. Mechanistically, cDC1s undergo mTOR inhibition, lysosome

hyperactivation, lysosomal membrane permeabilization (LMP) and apoptotic death. Surprisingly, computational and experimental methodologies collectively point to type I interferons as key inducers of LMP and cDC1 death within tumors. Thus, cDC1 apoptosis downstream of type I IFN signaling eliminates cDC1s in tumors. Current strategies to augment the tumor cDC1 pool are directed in enhancing cDC progenitor divergence to cDC1s [34]. Our studies propose LMP prevention as a rational approach to treat cDC1 deserts, increase immunotherapy responses and clinical outcomes.

RESULTS

Common gene expression modules among lung tumor cDC1s across different models point to lysosomal hyperactive states.

To decode the complexity of tumor-induced cDC1 states we leveraged orthotopic lung cancer models. These models develop solitary lung tumors rather than pulmonary nodules and thus allow tumor excision and sorting of pure tumor-infiltrating cells. To characterize the identity of lung tumor cDC1s in our model systems we digested murine lung tumors and healthy lungs and performed FACS analysis. We concatenated lineage negative, MHCII+CD11c+ cDCs of tumor and healthy samples and performed dimensionality reduction and unbiased clustering using MHCII, CD11C, CD11b and XCR1 as input. cDCs separated in 4 clusters: an XCR1^{high}CD11b^{-} bona fide cDC1s, XCR1^{-}CD11b^{+} bona fide cDC2 and two intermediate states XCR1^{low}CDC11b^{-} (XCR1^{low} mReg cDC) and XCR1^{-}CD11b^{-} (XCR1^{-}mReg cDC), likely corresponding to the previously described mRegs and DC3 **(Fig. 1a)**. Similar to what has been previously reported, bona fide tumor infiltrating cDC1s were less in lung tumors versus healthy lungs **(Fig. 1a)** [23]. cDC1 ablation and conditional gene knockout experiments have validated in vivo the key role of cDC1s in cancer immunity and immunotherapy. We recently developed a cDC1 specific XCR1^{cre} line in which a Cre recombinase and a fluorescent reporter are coexpressed under the control of the Xcr1 gene, in a manner that maintains XCR1 expression [12]. We crossed the Xcr1cre line with a loxP-STOP-loxP DTA line to constitutively delete cDC1s and analyzed tumor cellular profiles and burden in two orthotopic lung cancer models of different aggressiveness and immunogenicity. LLC tumors are less immunogenic, grow fast and mice succumb at ~ 2 weeks, while CULA tumors are more immunogenic, grow slow and mice succumb at ~4 weeks **(Suppl. Fig. 1)**. To monitor cancer antigen specific responses and quantify tumor burden we transduced both lines with fluorescent ovalbumin viral vectors. An extensive flow cytometry analysis using panels of markers against major myeloid and lymphoid subsets revealed a decrease in intratumoral CD4 and CD8 T cells, which was more prominent in the more immunogenic CULA tumors **(Suppl. Fig. 2 and Fig 1b)**. Staining with SIINFEKL-k^{b} tetramers that recognise ovalbumin-specific CD8+ T cells, indicated that cDC1 ablation almost completely abolished cancer-specific T cytotoxic cells in the CULA model and less in the LLC model **(Fig. 1b)**. These immunological defects were accompanied by a significant increase in tumor burden **(Fig. 1b)**. Thus, lung tumor growth requires cDC1 scarcity and there is a positive link between tumor immunogenicity and host dependence on cDC1s for immune rejection.

In the era of omics, it remains uncertain whether and how tumor cDC1s transcriptionally differ from their healthy counterparts [16, 26-29]. Single-cell methods inherently suffer from limitations in the recovery of complete transcriptomes due to the prevalence of transcriptional dropout events. To get a higher resolution on bona fide cDC1s in tumor versus healthy states we analyzed by bulk RNAseq XCR1^{high}CD11b^{neg} cDC1s purified from LLC and CULA lung tumors versus healthy lungs. A total of 9.720 genes were identified. Principal Components Analysis (PCA) showed that tumor and healthy cDCs1 separate in two distinct clusters **(Fig. 1c)**. One outlier sample was excluded for further analysis. Surprisingly, differential expression analysis found only 30 genes that were highly up-regulated (FDR<0.05) in tumor derived cDCs1 and 10 that were highly downregulated, in comparison with healthy cDC1s. Among top up regulated were genes involved in lysosomal processes (CD63, Gga2, Ctsd, Lgmn, Gpnmb), the well-known inhibitory molecule PDL1 and genes mediating interferon responses (Gbp2, Gbp5, Gbp7, Stat1, Irf1), while among top down regulated were genes involved in cell structure and adhesion (Pdlim1, Ahnak, CD44, Serpinb8) **(Fig. 1d)**. Interestingly, LLC tumor cDC1s showed a more robust tumor associated profile compared to CULA tumor cDC1s. It is tempting to speculate that this is linked to the higher aggressiveness of LLC tumors. Likewise, pathway activities of up-regulated genes analyzed by DAVID showed significant enrichment in type I and II IFNs and in lysosomal activities in cDC1s from tumors **(Fig. 1e)**. To validate our findings, we re-analyzed a publicly available scRNAseq dataset from cDCs that had been purified from a metastatic lung cancer model with a Kras^{G12D}P53$^{-/-}$ cell line. We filtered out from our analysis cDCs2 and mReg DCs and focused on the cDC1 annotated cluster. Two large (C1, C2) and two small cDC1 sub-clusters (C3, C4) were identified by uniform manifold projection (UMAP). The C1 sub-cluster was almost exclusively derived from the tumor-bearing lungs, while C2 from healthy lungs. **(Fig. 1f)**. Functional enrichment analysis of upregulated genes performed by DAVID showed significant enrichment in lysosomal processes and type I IFN pathways in C1 **(Fig. 1g)**. Pearson correlation analysis of commonly expressed genes between murine and bulk RNAseq datasets pointed to lysosome (Ctsd, CD63, Gbnmb) and IFN (Gbp2, IRF, Stat1) related genes as the most highly positively correlated **(Fig. 1h)**. Accordingly, top enriched GO terms/KEGG pathways were highly concordant between bulk and scRNAseq datasets **(Fig. 1i)**. Collectively, two independent datasets across 2 different lung cancer models and three different cancer lines show that tumor cDC1s become transcriptionally biased towards lysosomal hyperactive states and indicate a profound IFN impact.

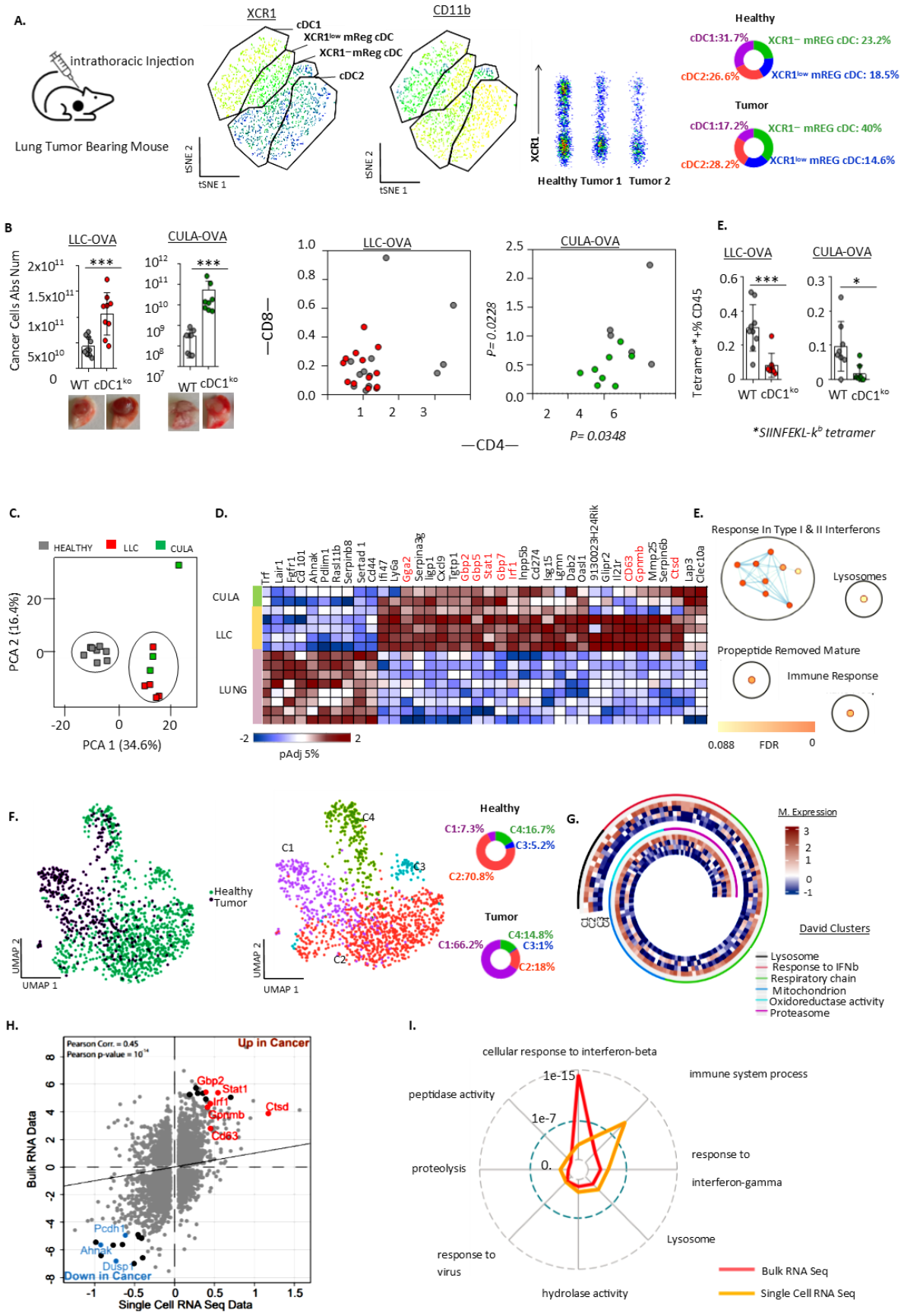
A.
intrathoracic Injection
Lung Tumor Bearing Mouse
XCR1
CD11b
cDC1
XCR1low mReg cDC
XCR1−mReg cDC
cDC2
tSNE 1
tSNE 2
Healthy Tumor 1 Tumor 2
Healthy
cDC1:31.7%
XCR1− mREG cDC: 23.2%
cDC2:26.6%
XCR1low mREG cDC: 18.5%
Tumor
cDC1:17.2%
XCR1− mREG cDC: 40%
cDC2:28.2%
XCR1low mREG cDC:14.6%
B
LLC-OVA
CULA-OVA
Cancer Cells Abs Num
WT cDC1ko
—CD8—
—CD4—
P= 0.0228
P= 0.0348
E.
Tetramer*+% CD45
*SIINFEKL-kb tetramer
C.
HEALTHY LLC CULA
PCA 2 (16.4%)
PCA 1 (34.6%)
D.
CULA
LLC
LUNG
pAdj 5%
Response In Type I & II Interferons
Lysosomes
Propeptide Removed Mature
Immune Response
FDR
F.
Healthy
Tumor
UMAP 1
UMAP 2
C1
C2
C3
C4
Healthy
C1:7.3%
C4:16.7%
C3:5.2%
C2:70.8%
Tumor
C4:14.8%
C3:1%
C1:66.2%
C2:18%
G.
M. Expression
David Clusters
Lysosome
Response to IFNb
Respiratory chain
Mitochondrion
Oxidoreductase activity
Proteasome
H.
Pearson Corr. = 0.45
Pearson p-value = 10^-14
Up in Cancer
Down in Cancer
Gbp2
Stat1
Irf1
Gpnmb
Cd63
Ctsd
Pcdh1
Ahnak
Dusp1
Bulk RNA Data
Single Cell RNA Seq Data
I.
cellular response to interferon-beta
immune system process
peptidase activity
proteolysis
response to interferon-gamma
Lysosome
response to virus
hydrolase activity
1e-15
1e-7
0.
Bulk RNA Seq
Single Cell RNA Seq

***Figure 1. cDC1-dependent cancer models point to lysosomal hyperactive states of tumor-infiltrating cDC1s. A**. The LLCmCherry cell line was orthotopically inoculated on the left lung lobe of Bl6 mice via direct intrathoracic injection. On day 12 tumors and healthy lungs from control mice were excised, digested, stained and analyzed by FACS. Fcs files from *lin^{-ve}CD11c^{+}MHCII^{+} cDCs were concatenated. t-SNE was run using XCR1, CD11b, MHCII and CD11c as input. **B**. The XCR1cre line was crossed to XCR1DTA to constitutively delete cDC1s (cDC1KO). Mice were inoculated with the LLC-OVA^{mCherry} or the less aggressive more immunogenic CULA-OVA^{mCherry} orthotopically. Tumors were excised on day 12 (LLC model) or day 28 (CULA model), digested, stained and analyzed by FACS. From left to right. Absolute number of mCherry cancer cells enumerated with facs counting beads. CD4^{+} and CD8^{+} T cells percent CD45^{+} cells. OVA-specific CD8^{+} T cells percent total CD8^{+} T cells, identified with SIINFELK-k^{b} tetramers. Data are pooled from two independent experiments. **C**. lin^{-ve}CD11c^{+}MHCII^{+}CD11b^{-}XCR1^{high} cDC1s were sorted from LLC-OVA or CULA-OVA lung tumors and healthy lungs. Bulk RNAseq was performed and data were analyzed by principal component analysis (PCA). **D**. Heatmap of the top differentially expressed genes. **E**. GO terms analysed by DAVID. **F**. UMAP of a murine cDC1 scRNAseq dataset[26]. Single cells originated from lungs bearing metastatic KP nodules and from healthy lungs. **G**. Heatmap depicts genes that were found enriched in pathway analysis performed by David. **H**. Pearson's correlation between the bulk RNAseq dataset (c,d,e) and the scRNAseq dataset (f,g). **I**. Common enriched pathways between the two datasets. *Lin:CD3,NK1.1,B220,CD11b,Ly6C,Ly6G. *P<0.05, ***P<0.001. Error bars, mean± sem; two-tailed unpaired t-test.*

mTOR inhibition induces lysosomal stress response in tumor cDC1s

To validate in vivo the functional profile that had been identified computationally, we repeated our orthotopic transplantation studies, excised tumors and labeled cells with a fluorescent lysosomal pH reporter (LysoTracker) and a fluorescent reporter of the activity of lysosomal proteases (DQ-BSA). FACS analysis showed an increase in lysosomal acidification and protease activities of tumor derived cDCs1 in comparison to healthy lung cDCs1 **(Fig 2a, 2b)**. These findings are consistent with the understanding that the activity of most lysosomal enzymes is positively regulated by acidic pH. Glycoprotein Non-metastatic Protein B (GPNMB), is known to be associated with endosomal/lysosomal structures in cells overexpressing the protein during stress conditions, characteristically in lysosomal storage disorders [31, 35]. Intracellular Gpnmb staining showed upregulation in tumor versus healthy lung cDC1s **(Fig. 2c)**. To sustain antigen stability, healthy cDC1s are less capable for lysosomal degradation [36]. To investigate whether activation of lysosomal proteases in tumor cDC1s enhanced their ability to degrade cancer antigens, we FACS-sorted tumor and healthy lung cDC1s and co-cultured them with tagged apoptotic LLC cells. The antigen load of both types of cDC1s peaked on the same day, but was consistently lower in tumor versus healthy cDC1s at different time points **(Fig. 2d)**. This was due to fast antigen degradation rather than low endocytosis, as an endocytosis fluorescent reporter (FITC-Dextran, 40.000 MW) showed no difference between lung tumor and healthy lung cDC1s **(Fig. 2e)**.

To investigate the mechanism by which tumors up-regulate lysosome acidification and function, we took a candidate-based approach and investigated mTORC1. Activation of mTORC1 occurs on lysosomes. When the levels of nutrient and inflammatory signals are high, the mTORC1 complex is recruited to the cytosolic face of lysosomal membranes [37, 38]. Once on the lysosomal surface, mTORC1 is activated. Different stimuli must cooperate in order to achieve full mTORC1 activation and phosphorylation of the lysosomal transcription factor TFEB, impeding its translocation to the nucleus [37, 38]. Starvation and oxidative stress inhibit mTORC1 activation, leading to TFEB dephosphorylation, its nucleus translocation and lysosome/lysosomal enzymes

biogenesis **(Fig. 2f)**. Phospho-FACS of orthotopic lung tumors versus healthy lungs showed an impressive decrease in phospho-mTOR in tumor cDC1s, while phospho-AKT and phospho-S6 two other mediators of the mTORC1 pathway remained unaltered **(Fig. 2f)**. To investigate whether inhibition of mTOR phosphorylation is causal to lysosomal activation in tumor microenvironments, we set up an ex vivo culture system using the Mutu cDC1 cell line. To recapitulate the complex molecular features of tumor and healthy lung microenvironments we cultured lung tumor and healthy lung tissue fragments, purified the Tumor Culture Medium (TCM) and Healthy Culture Medium (HCM) and used them as supplements to Mutu cDC1 cultures. Phospho-mTOR was significantly less in the presence of TCM versus HCM, and this was accompanied by enhanced lysosomal acidification and Gbnmb up-regulation **(Fig. 2g)**. Importantly, in the presence of the mTOR activator bafilomycin A1 the TCM lost its ability to activate lysosomal processes in cDC1s **(Fig. 2g)**. Thus, signals in the tumor microenvironment prevent mTOR activation in cDC1s, leading to lysosomal acidification and fast antigen degradation.

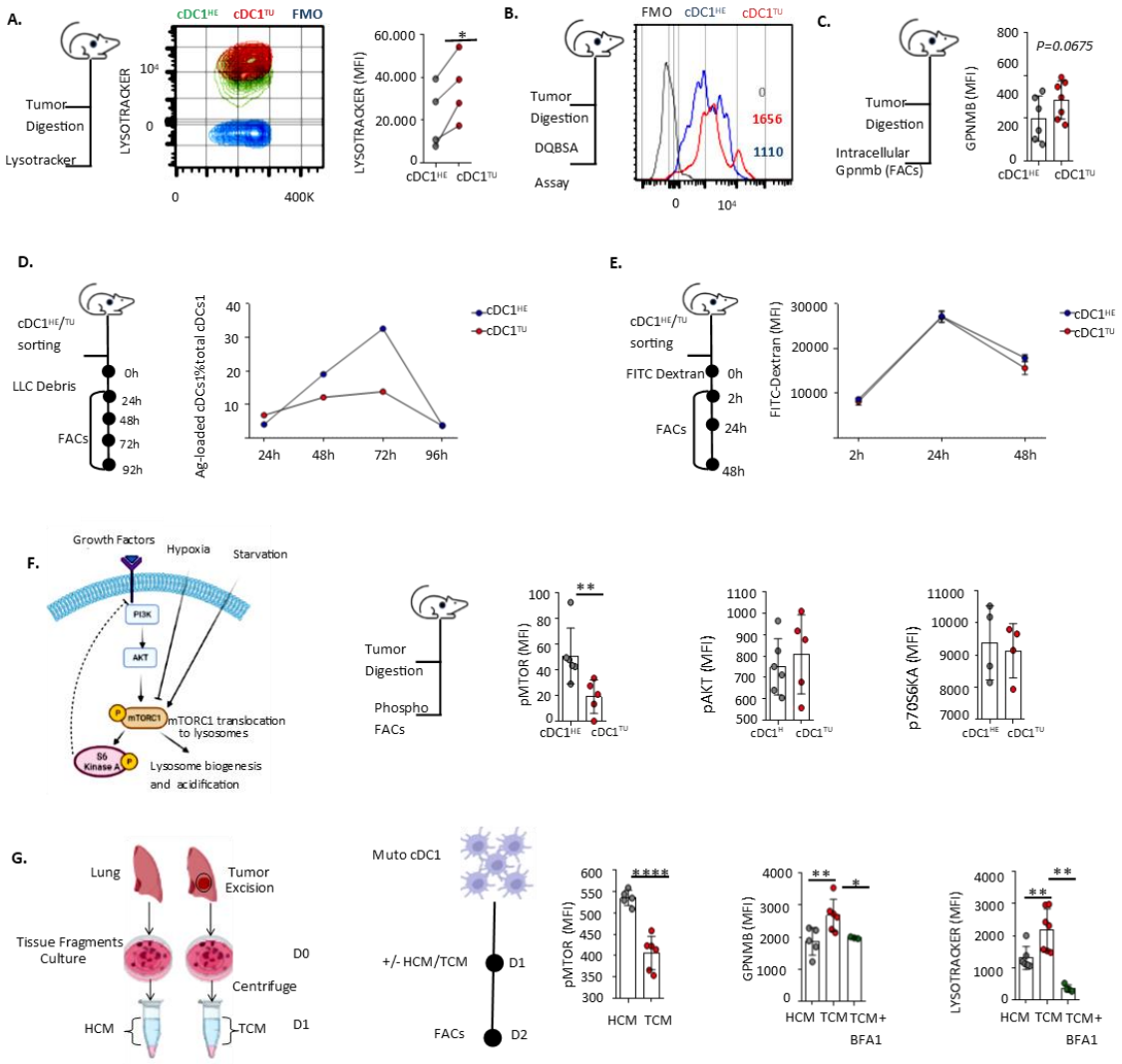

Figure 2. Tumors inhibit phosphorylation of cDC1 mTOR leading to lysosomal stress. A-F. *The LLC cell line was orthotopically inoculated on the left lung lobe of Bl6 mice via direct intrathoracic injection. On day 12 tumors and healthy lungs from control mice were excised and digested to obtain single cell suspensions.* ***A****. Lysotracker and antibody stains were performed and analysed by facs. Graph depicts LysoTracker MFI of Lin^{-}MHCII^{+}CD11c^{+}CD11b^{-} XCR1^{high} cDC1s. Data are representative of three independent experiments.* ***B****. Cells were cultured with fluorescent DQ-BSA for 24 hours, stained with antibodies and analysed by facs. Histograms are gated on XCR1^{high} cDC1s. Data are representative of two independent experiments.* ***C****. Intracellular staining for Gpnmb. Graph depicts Gpnmb MFI of cDC1s. Data were pooled from two independent experiments.* ***D****. XCR1^{high} cDC1s were sorted and cultured with apoptotic fluorescent LLC cells for 4 days. At the indicated time points they were analysed by facs. Graph depicts LLC loaded cDC1s percent total cDC1s. Data are representative of two independent experiment.* ***E****. XCR1^{high} cDC1s were sorted and cultured with fluorescent Dextran for 2 days. At the indicated time points they were analysed by facs. Graph depicts cDC1s that have endocytosed Dextran percent total cDC1s. Data were pooled of two independent experiments.* ***F****. From left to right. Graphical summary of the mTORC1 pathway. Antibody stains against phospho-proteins were performed and analysed by facs. Graph depicts MFI of XCR1^{high} cDC1s. Data are pooled from two independent experiments.* ***G****. Tumor tissue and healthy lungs were chopped and fragments were cultured for 24h. Tumor culture medium (TCM) and Healthy Culture Medium (HCM) were purified and added to the Mutu cDC1 line. After 24h the Mutu was analysed by phospho-stain for pMTOR, LysoTracker stain and Gpnmb intracellular stain. Data were pooled from two independent experiments.*P<0.05, **P<0.01. ***P<0.0001 Error bars, mean± sem; two-tailed unpaired or paired t-test.*

Lysosomal activation depends on inhibition of mTOR phosphorylation downstream of INFRA1 signaling.

To reconstruct the regulatory networks that drive lysosomal states in tumors we performed regulon inference using the scalable SCENIC platform in the murine scRNAseq dataset. The activity of the predicted regulons in all individual cDC1s was quantified and cellular AUCs were used as input for UMAP visualization and clustering. Impressively, the SCENIC AUC UMAP clearly separated a tumor-specific cDC1 cluster that almost completely overlapped with the C1 tumor-specific cluster in the transcriptome UMAP **(Fig. 3a)**. Ranking all regulons of the tumor C1 cluster according to the regulon specificity score pointed to STAT1 and STAT2 as the top regulons **(Fig. 3b)**. The transcription factors STAT1 and STAT2 are key mediators of type I and type II IFN signaling. Thus, our regulon analysis points to IFNs as inducers of the observed tumor cDC1 states.

IFNs drive cDC1 maturation and migration and are critical determinants of anti-tumor immunity and clinical outcomes [39]. IFNs regulate mTOR phosphorylation, but positive as well as negative effects have been reported depending on cell type and context [40, 41], with data on cDC1 lacking. To investigate changes in the mTOR and lysosomes driven by types I (IFNa, IFNb) and type II IFNs (IFNg), we performed in vitro assays with the Mutu cDC1 line. Exposure of Mutu cDC1s to pure IFNa and IFNb, but not IFNg induced a simultaneous increase in Gpnmb expression and lysosomal acidification **(Fig. 3c)**. Both responses were abrogated in the presence of the mTOR activator Bafilomycin A1 **(Fig. 3c)**. Thus, type I IFNs activate lysosomes of Mutu cDC1s via mTOR inhibition. To investigate whether type I IFNs in tumors activated the lysosomes of cDC1s in vivo, we developed mixed bone marrow chimeras by sub-lethal irradiation and transplantation of CD45.1 wild type and CD45.2 INFRA1 knockout bone marrow cells at a 1:1 ratio **(Fig. 3d)**. Chimeric mice were subjected to lung transplantation of LLC cells, tumors were excised and analyzed by FACS, gating on CD45.1 wild type versus CD45.2 INFRA1 knockout cDC1s. INFRA1 depleted intratumoral cDC1s showed decreased lysosomal acidification compared to wild type cDC1s **(Fig. 3e)** and higher levels of mTOR phosphorylation **(Fig. 3f)**. Thus, taken together

with the aforementioned computational analysis the cytokine exposure testings and the in vivo receptor perturbations, they all point to type I IFNs as inducers of activated cDC1 lysosomal states in tumors via mTOR inhibition.

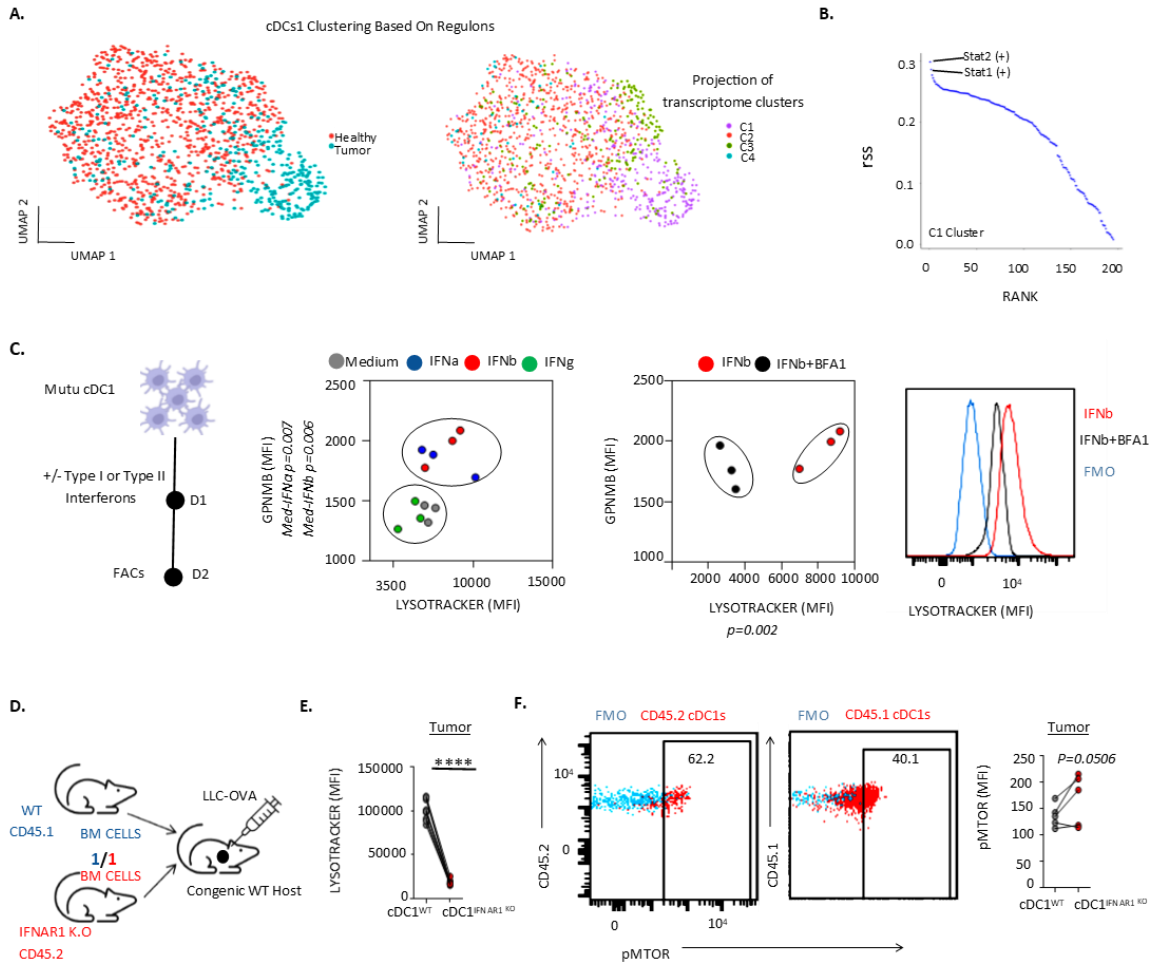

Figure 3. Type I IFNs inhibit mTOR phosphorylation to activate lysosomes of tumor cDC1s. ***A****. SCENIC AUC UMAPs of a murine cDC1 scRNAseq dataset [26]. Single cells originated from lungs bearing metastatic KP nodules and from healthy lungs. The activity of the predicted regulons in all individual cDC1s was quantified and cellular AUCs were used as input for UMAP Left: Color-coded based on tumors vs healthy cDC1s, Right: Color-coded based on transcriptome clusters (Fig.1f).* ***B.*** *Ranking of the regulon specificity scores of the tumor cluster.* ***C****. The Mutu cDC1 line was cultured as depicted in the scheme. The Bafilomycin A1 mTOR activator was added in selected experiments. After 24h cells were subjected to LysoTracker stain or to intracellular Gpnmb stain. Data are representative of two independent experiments.* ***D-F****. CD45.1 wild type / CD45.2 INFRA1 knockout mixed bone marrow chimeras were subjected to lung transplantation of LLC cells. On day 12 tumors were excised, digested and single cells were obtained.* ***D****. Graphical scheme.* ***E****. Single cells were stained with LysoTracker and antibodies. Graphs depict LysoTraker MFI of CD45.1 wild type versus CD45.2 INFRA1 knockout XCR1^{+} cDC1s. Data are representative of two independent experiments.* ***F****. Single cells were subjected to phospho-mTOR and antibody stains. Graphs depict pMTOR MFI of CD45.1 wild type versus CD45.2 INFRA1 knockout XCR1^{+} cDC1. Data are representative of two independent experiments. **P<0.01.****.P<0.0001 Error bars, mean± sem; two-tailed paired t-test.*

IFN-induced lysosomal stress breaches the lysosome-to-cytosol barrier causing apoptotic death in tumor cDC1.

Lysosomal activity is essential to preserve cellular homeostasis and lysosomal dysfunction has been implicated in various diseases. Lysosomal stress can induce lysosomal membrane permeabilization (LMP), resulting in the translocation to the cytoplasm of intralysosomal enzymes, such as cathepsins, inducing lysosomal-dependent cell death (LDCD) [42]. We hypothesized that cDC1 deserts in tumors may be due to LDCD. In primary tissues quantification of late apoptotic dead cDC1s is not feasible, because cDC1 specific antibodies tend to non-specifically bind to all dead cells. Quantification of early apoptotic Annexin V positive live cells by FACS pointed to a higher number of early apoptotic cDC1s in lung tumors versus healthy lungs **(Fig. 4a)**. To validate these findings in another experimental setting we exposed Mutu cDC1s to tumor versus healthy culture medium and morphologically quantified apoptotic cells by creating a forward scatter (FS) / side scatter (SS) apoptotic cell gate or performed Annexin V staining **(Figs. 4b, 4c).** Tumor culture medium induced Mutu cDC1 apoptosis and this was replicated by exposure to IFNa, IFNb, but not IFNg **(Figs. 4b, 4c)**. These findings suggested that type I IFNs in tumors induce cDC1 apoptosis. Impressively, only 20% of cDC1s that were found in lung tumors of wild type mice were NFRA1 positive, while NFRA1 positive cDC1s infiltrating healthy lungs were over 60% **(Fig. 4d)**. Thus, cDC1 tumor deserts are associated with selective depletion of INFRA1 expressing subsets. To directly show in vivo that type I IFNs induce cDC1 apoptosis in tumors, we revisited our mixed bone marrow chimeric models. CD45.1 wild type / CD45.2 INFRA1 knockout chimeric mice were subjected to lung transplantation of LLC cells, tumors were excised and analyzed by FACS, gating on CD45.1 wild type versus CD45.2 INFRA1 knockout cDC1s. INFRA1 knockout cDC1s, but not all INFRA1 hematopoietic cells, significantly outnumbered wild type cDC1s in tumors **(Fig. 4e)**. Accordingly, the percentage of early apoptotic cDC1s was higher among WT versus INFRA1 knockout cDC1s and this accompanied by an increased number of live NFRA1 knockout versus wild type cDC1s in tumors **(Fig. 4e)**. Collectively, in vivo and ex vivo assays suggest that type I IFN-induced cDC1 apoptosis causes cDC1 scarcity in tumors. To detect whether type I IFNs could cause LMP in cDC1s, we exposed the Mutu cDC1 line to tumor versus healthy culture medium (TCM vs HCM) and imaged cathepsin D by immunofluorescence. Cathepsin D localized outside lysosomes into the cytoplasm of Mutu cDC1s that had been exposed to TCM but inside the lysosomes of Mutu cDC1s that had been exposed to HCM (**Fig. 4f)**. Detection of galectin puncta at leaky lysosomes is another highly sensitive assay for LMP. To investigate whether LMP happened *in vivo* in tumors as a result of type I IFNS, we inoculated again LLC cells in our mixed CD45.1 wild type / CD45.2 INFRA1 KO chimeras, sorted CD45.1 versus CD45.2 tumor-infiltraing cDC1s and stained them for galectin3. Galectin3 formed puncta around the nucleus and on the membrane of lysosomes of wild type, but not IFAR1 KO cDC1s **(Fig. 4g)**. Collectively, our data suggest that type I IFNs induce LMP and LDCD in tumor cDC1s, which may cause cDC1.

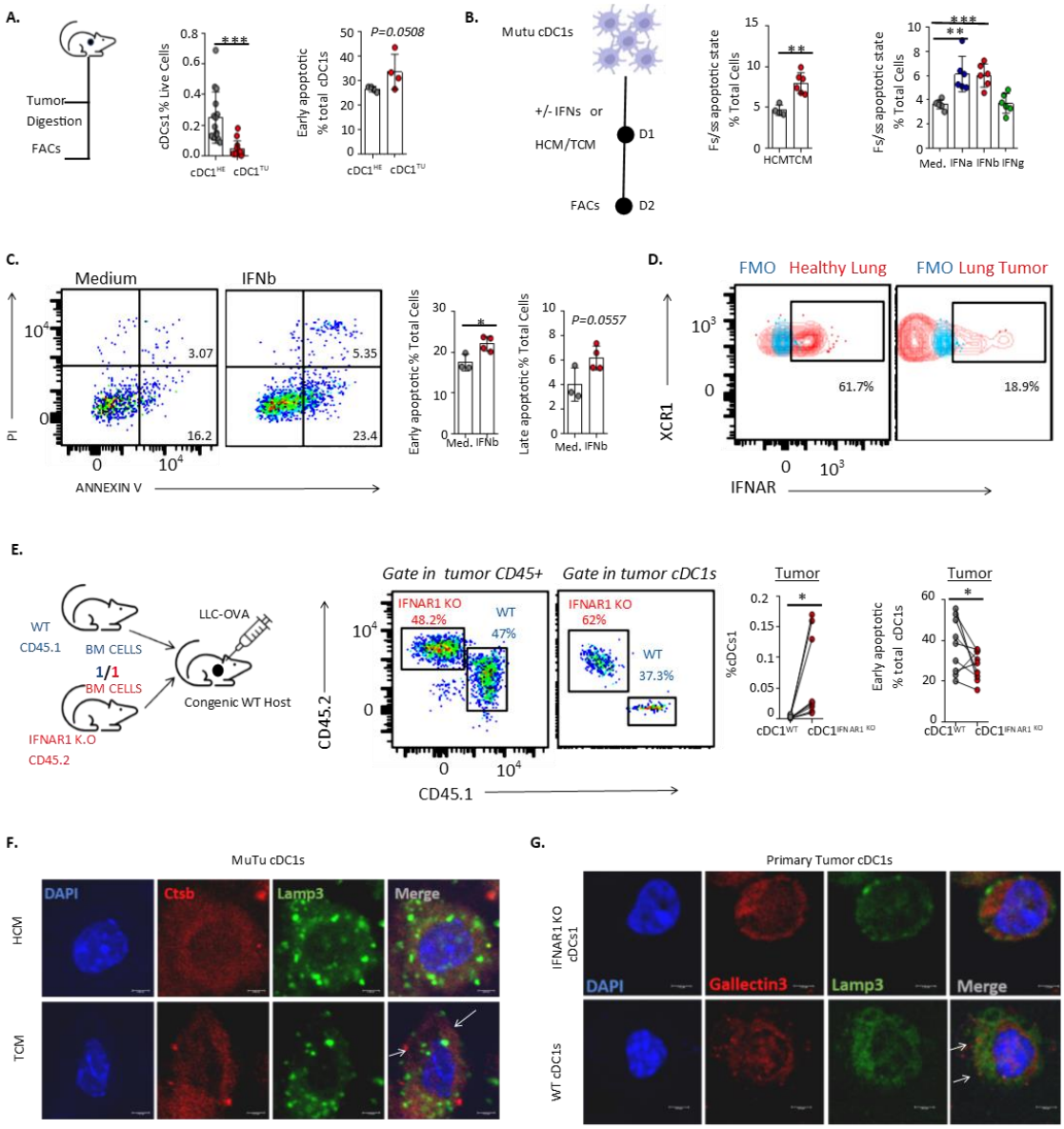

Figure 4. Type I IFNs induce lysosomal membrane permeabilization and lysosomal dependent cell death. A*. The LLC cell line was orthotopically inoculated on the left lung lobe of Bl6 mice via direct intrathoracic injection. On day 12 tumors and healthy lungs from control mice were excised and digested to obtain single cell suspensions. Annexin V and antibody stains were performed and analysed by facs. From left to right. Graphical scheme. Live cDC1s percent total cells. Early apoptotic (annexin V^+PI^-) cDC1s percent cDC1s. Data were pooled from two independent experiments,* ***B,C****. Tumor tissue and healthy lungs were chopped and fragments were cultured for 24h. Tumor culture medium (TCM) and Healthy Culture Medium (HCM) were purified and added to the Mutu cDC1 line. Alternatively, the Mutu line was exposed to pure IFNs, as depicted. After 24h FACS analysis was performed.* ***B.*** *Apoptotic FS/SS gate percent total cDC1s. Data were pooled from three independent experiments.****C****. Early apoptotic (annexin V^+PI^-) and late apoptotic (annexin V^+ PI^+) percent total cells. Data are representative of two independent experiment.* ***D.*** *As in A. Graphs are gated in $XCR1^{high}$cDC1s. Data are representative of two independent experiments .****E****. CD45.1 wild type / CD45.2 INFRA1 knockout mixed bone marrow chimeras were subjected to lung transplantation of LLC cells. On day 12 tumors were excised, digested and single cells were obtained. From left to right. FACS plot depicts CD45.1/CD45.2 expression gated in $XCR1^{high}$ cDC1s. Dotplots show live cDC1s percent total cells and early apoptotic (Annexin V+ PI^-) cDC1s percent total cDC1s. Data were pooled from two independent experiments. F. IF*

stain of cathepsin b (CTSb) and Lamp3 in Mutu cells upon exposure to HCM/TCM. Data were representative of two independent experiments. ***G****. Experimental design as in E. Intratumoral CD45.1 WT versus CD45. 2 INFAR1 cDC1s were sorted and analysed by immunofluoresence. Gallectin puncta was imaged by Gallectin3, Lamp3 c-stain. Data were representative of two independent experiments. *P<0.05, **P<0.01. ***P<0.001 Error bars, mean± sem; two-tailed unpaired or paired t-test.*

Lysosome damage and IFN responses align across human and murine tumor cDCs1. Humans are much more diverse and heterogeneous compared to laboratory mice. To investigate the translatability of our murine studies in the human system we leveraged a publicly available mega-integrated dataset consisting of 178,651 human mononuclear phagocytes from 13 tissues across 41 datasets[43]. We filtered out non-cancer patients and patients with malignancies of lymphoid tissues, leaving us with 2315 annotated cDC1s across 39 paired human and cancer samples of the liver, lung, colon and kidney. cDC1 percent total mononuclear phagocytes were decreased in lung, colon and kidney tumor versus healthy samples, suggesting cDC1 tumor deserts might be found across different tissues and patients **(Fig.5a)** . Dimensionality reduction using UMAP showed that cDC1s cluster predominately by tissue of origin rather than tumor versus healthy state **(Fig. 5b)**. Differential expression analysis between tumor and healthy state revealed a relatively small number of de-regulated genes. Strikingly, among the few genes that were up-regulated were IFN-inducible genes (STAT1, GBP2) and cathepsin (CTSA, CTSD) **(Fig. 5c)**. Accordingly, pathway analysis showed significant enrichment in GO terms and KEGG pathways related to IFNs and lysosomes **(Fig. 5d)**. Importantly, apoptotic pathways were also found enriched **(Fig 5d)**. Regulon inference using the SCENIC algorithm, unraveled STAT1 as top specific regulon of tumor cDC1 state **(Fig 5e.)**. Overall, human tumor cDC1 states are concordant with those of mice, both characterized by intertwined IFN-lysosome-apoptosis functional modules.

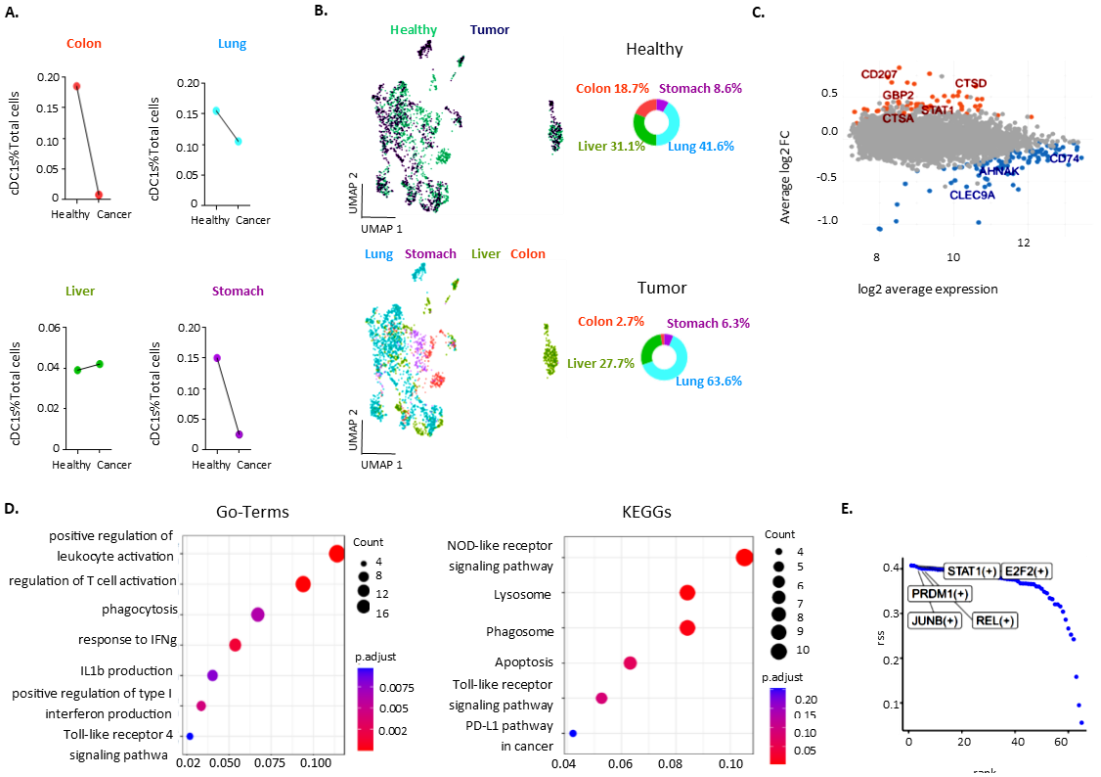

Figure 5. Pathway analysis across human cancer cDC1s point to an intertwined IFN-lysosome-apoptosis triad. A*. A publicly available scRNAseq dataset consisting of mononuclear phagocytes of paired tumor/healthy tissues samples was downloaded [43]. Single cells annotated as cDC1 in each tissue were expressed as percent of total mononuclear phagocytes sequenced in the same tissue.* ***B.*** *UMAP clustering.* ***C****. MA plot showing top deregulated genes of interest (highlighted FDR<0.05).* ***D****. Pathway analysis performed by David.* ***E.*** *Ranking of tumor cDC1 regulons (SCENIC) according to their regulon specificity score (RSS).*

Discussion

There is abundant evidence that cDC1s become extremely scarce in solid tumors. However, mechanistic understanding is incomplete. Here we uncovered an unexpected role of type I IFNs in cDC1 extinction from tumor sites. We demonstrate the following: i) tumor tissues induce lysosome biogenesis, acidification and proteolysis in cDC1s, ii) mTOR activation prevents tumor-induced lysosomal responses, iii) the type I IFN-induced NFRA1 signaling pathway lies upstream of mTOR inhibition and lysosome activation, iv) type I IFNs induce cDC1 apoptotic death in tumors, v) type I IFN tumor-induced apoptosis is accompanied by permeabilization of the lysosomal membrane of cDC1s. Our studies do not and wish not reject the important role of impaired cDC1 recruitment at tumor sites. In fact, we believe that LDCD amplifies the impact of low recruitment rates resulting in cDC1 deserts in tumors.

LDCD is a cell death pathway that involves LMP and the release of cathepsins into the cytosol [37, 42]. In some other instances, LMP and cathepsin engage effectors that result in apoptosis [37, 42]. Type I IFN induced lysosomal acidification and increased proteolysis are also seen in Salmonella-infected epithelial cells, leading to rupture of Salmonella-containing vacuoles, pathogen exposure to the cytosol and epithelial cell death [44]. Thus, type I IFNs may activate lysosomal processes of several cell types and many disease contexts. LMP and lysosomal stress can inhibit the mTORC1 pathway as a compensatory mechanism, in order to enhance lysosome biogenesis [37, 42]. In our models, IFNb-induced activation of cDC1 lysosomes was prevented by the mTOR activator Bafilomycin, suggesting mTOR lies upstream of lysosomal activation. Considering that AKT phosphorylation did not differ between healthy and tumor cDC1s, mTOR inhibition is likely AKT-independent. Thus, our data point to a yet unknown inhibitory intersection between the type I IFN and mTORC1 pathways.

There are numerous and contrasting reports on the effects of mTOR in cDC endocytosis, maturation, LN migration and antigen presentation, both in homeostasis and upon infection[39]. A new picture has emerged, whereby the net immunological outcome of mTOR regulation depends on the spatiotemporal context [39]. The mTOR phosphorylation status of cDCs in tumors is largely unknown. Opposing stimuli, such as inflammatory signals and nutrient deprivation, are expected to compete in activating and inhibiting mTOR, respectively. Our in vitro and in vivo perturbation experiments convincingly show that for cDC1s the balance in tumor microenvironments shifts towards mTOR inhibition. It is very likely, however, that tumor starvation acts in parallel to type I IFN signaling to inhibit mTOR.

LMP is induced by lysosomal destabilization in the presence of pore-forming molecules, such as Bax and Bac [37, 42]. We did not exactly show how pores are forming in the membrane of cDC1s, but besides Bax and Bac, more interesting and novel candidates are the Gbp family of proteins. These IFN-induced GDPases are known to form supramolecular complexes on the membrane of pathogen-containing vacuoles, leading to vacuolar lysis, but have never been related to LMP and LDCD to date [45]. We found them highly up-regulated in murine and human cDC1s across several cancers and we are currently exploring whether they mediate the lysis of the membrane of the stressed cDC1 lysosomes.

A recent study reported a progressive decrease in cDC1s in tumor draining LNs and indicated a decrease in cDC1 migration rates through unknown mechanisms [26]. We have uncovered three factors that can all change the cytoskeleton dynamics and calcium signaling of cDC1s and thus may impede their migration to LNs[46]: lysosomal stress [47, 48], early apoptosis [49] and increased GBPs [50]. Interestingly, among the top down-regulated genes in tumor cDC1s there were several related to cytoskeleton and cell adhesion, further substantiating such a hypothesis.

Albeit recently accused for secondary resistance to immunotherapy, type I IFNs are well known for their anti-tumor functions[51]. They specifically keep cDCs at a poised homeostatic state [52] and stimulate cDC maturation and LN migration upon perturbation. Thus, it is difficult to envisage a therapeutic scenario whereby targeting IFNs per se to prevent cDC1 LMP will ameliorate clinical outcomes of cancer patients. There are already research efforts to directly target LMP to treat lysosomal storage disorders [42]. Such drugs could be also re-purposed to prevent cDC1 LMP in tumors. Delineating the mechanism of pore formation in cDC1 lysosomes may also reveal novel therapeutic targets. Thus, our studies have i) explained the cDC1 deserts in tumors via the LDCD, ii) uncovered an inhibitory mTOR pathway downstream of type I IFNs that leads to LDCD, iii) pointed a research avenue that may lead to novel immunotherapeutic targets.

AKNOWLEDGEMENTS We would like to thank D. Konstantopoulos for sharing expertise in the computational analysis. We acknowledge G. Kollias, E. Andreakos, and G. Stathopoulos for sharing mouse models, cell lines and protocols. The NIH Tetramer Core Facility for SIINFEKL tetramers. We thank BSRC “Al. Fleming” flow cytometry, animal house, imaging and genomics facilities and the bioinformatics facility of “The Greek Research Infrastructure for Personalised Medicine (pMedGR)” (MIS 5002802).

CONTRIBUTIONS Conception, study design, M.T.; Development of methodology, M.T., E.A., B.M., S.H.; Acquisition of data, E.A., A.C., D.K., I.A. and M.M..; Analysis and interpretation of data, M.T., E.A., B.M., and S.H.; Writing the manuscript, M.T.; Preparing the figures, E.A. and A.C.; Study supervision, M.T.

REFERENCES

1. Eisenbarth, S.C., *Dendritic cell subsets in T cell programming: location dictates function.* Nat Rev Immunol, 2019. **19**(2): p. 89-103.
2. Kambayashi, T. and T.M. Laufer, *Atypical MHC class II-expressing antigen-presenting cells: can anything replace a dendritic cell?* Nat Rev Immunol, 2014. **14**(11): p. 719-30.
3. Cabeza-Cabrerizo, M., et al., *Dendritic Cells Revisited.* Annu Rev Immunol, 2021. **39**: p. 131-166.
4. Durai, V. and K.M. Murphy, *Functions of Murine Dendritic Cells.* Immunity, 2016. **45**(4): p. 719-736.
5. Eickhoff, S., et al., *Robust Anti-viral Immunity Requires Multiple Distinct T Cell-Dendritic Cell Interactions.* Cell, 2015. **162**(6): p. 1322-37.
6. Hor, J.L., et al., *Spatiotemporally Distinct Interactions with Dendritic Cell Subsets Facilitates CD4+ and CD8+ T Cell Activation to Localized Viral Infection.* Immunity, 2015. **43**(3): p. 554-65.
7. Steinman, R.M., *Decisions about dendritic cells: past, present, and future.* Annu Rev Immunol, 2012. **30**: p. 1-22.
8. Broz, M.L., et al., *Dissecting the tumor myeloid compartment reveals rare activating antigen-presenting cells critical for T cell immunity.* Cancer Cell, 2014. **26**(5): p. 638-52.
9. Ferris, S.T., et al., *cDC1 prime and are licensed by CD4(+) T cells to induce anti-tumour immunity.* Nature, 2020. **584**(7822): p. 624-629.
10. Roberts, E.W., et al., *Critical Role for CD103(+)/CD141(+) Dendritic Cells Bearing CCR7 for Tumor Antigen Trafficking and Priming of T Cell Immunity in Melanoma.* Cancer Cell, 2016. **30**(2): p. 324-336.
11. Ruhland, M.K., et al., *Visualizing Synaptic Transfer of Tumor Antigens among Dendritic Cells.* Cancer Cell, 2020. **37**(6): p. 786-799 e5.
12. Wohn, C., et al., *Absence of MHC class II on cDC1 dendritic cells triggers fatal autoimmunity to a cross-presented self-antigen.* Sci Immunol, 2020. **5**(45).
13. Murphy, T.L. and K.M. Murphy, *Dendritic cells in cancer immunology.* Cell Mol Immunol, 2022. **19**(1): p. 3-13.
14. Barry, K.C., et al., *A natural killer-dendritic cell axis defines checkpoint therapy-responsive tumor microenvironments.* Nat Med, 2018. **24**(8): p. 1178-1191.
15. Bottcher, J.P., et al., *NK Cells Stimulate Recruitment of cDC1 into the Tumor Microenvironment Promoting Cancer Immune Control.* Cell, 2018. **172**(5): p. 1022-1037 e14.
16. Michea, P., et al., *Adjustment of dendritic cells to the breast-cancer microenvironment is subset specific.* Nat Immunol, 2018. **19**(8): p. 885-897.
17. Ghislat, G., et al., *NF-kappaB-dependent IRF1 activation programs cDC1 dendritic cells to drive antitumor immunity.* Sci Immunol, 2021. **6**(61).
18. Hildner, K., et al., *Batf3 deficiency reveals a critical role for CD8alpha+ dendritic cells in cytotoxic T cell immunity.* Science, 2008. **322**(5904): p. 1097-100.
19. Garris, C.S., et al., *Successful Anti-PD-1 Cancer Immunotherapy Requires T Cell-Dendritic Cell Crosstalk Involving the Cytokines IFN-gamma and IL-12.* Immunity, 2018. **49**(6): p. 1148-1161 e7.
20. Salmon, H., et al., *Expansion and Activation of CD103(+) Dendritic Cell Progenitors at the Tumor Site Enhances Tumor Responses to Therapeutic PD-L1 and BRAF Inhibition.* Immunity, 2016. **44**(4): p. 924-38.
21. Sanchez-Paulete, A.R., et al., *Cancer Immunotherapy with Immunomodulatory Anti-CD137 and Anti-PD-1 Monoclonal Antibodies Requires BATF3-Dependent Dendritic Cells.* Cancer Discov, 2016. **6**(1): p. 71-9.
22. Lam, K.C., et al., *Microbiota triggers STING-type I IFN-dependent monocyte reprogramming of the tumor microenvironment.* Cell, 2021. **184**(21): p. 5338-5356 e21.
23. Lavin, Y., et al., *Innate Immune Landscape in Early Lung Adenocarcinoma by Paired Single-Cell Analyses.* Cell, 2017. **169**(4): p. 750-765 e17.
24. Hegde, S., et al., *Dendritic Cell Paucity Leads to Dysfunctional Immune Surveillance in Pancreatic Cancer.* Cancer Cell, 2020. **37**(3): p. 289-307 e9.
25. Gerhard, G.M., et al., *Tumor-infiltrating dendritic cell states are conserved across solid human cancers.* J Exp Med, 2021. **218**(1).
26. Schenkel, J.M., et al., *Conventional type I dendritic cells maintain a reservoir of proliferative tumor-antigen specific TCF-1(+) CD8(+) T cells in tumor-draining lymph nodes.* Immunity, 2021. **54**(10): p. 2338-2353 e6.
27. Cheng, S., et al., *A pan-cancer single-cell transcriptional atlas of tumor infiltrating myeloid cells.* Cell, 2021. **184**(3): p. 792-809 e23.

28. Di Pilato, M., et al., *CXCR6 positions cytotoxic T cells to receive critical survival signals in the tumor microenvironment.* Cell, 2021. **184**(17): p. 4512-4530 e22.
29. Zilionis, R., et al., *Single-Cell Transcriptomics of Human and Mouse Lung Cancers Reveals Conserved Myeloid Populations across Individuals and Species.* Immunity, 2019. **50**(5): p. 1317-1334 e10.
30. Meyer, M.A., et al., *Breast and pancreatic cancer interrupt IRF8-dependent dendritic cell development to overcome immune surveillance.* Nat Commun, 2018. **9**(1): p. 1250.
31. Saade, M., et al., *The Role of GPNMB in Inflammation.* Front Immunol, 2021. **12**: p. 674739.
32. Zelenay, S., et al., *Cyclooxygenase-Dependent Tumor Growth through Evasion of Immunity.* Cell, 2015. **162**(6): p. 1257-70.
33. Spranger, S., R. Bao, and T.F. Gajewski, *Melanoma-intrinsic beta-catenin signalling prevents anti-tumour immunity.* Nature, 2015. **523**(7559): p. 231-5.
34. Wilson, K.R., J.A. Villadangos, and J.D. Mintern, *Dendritic cell Flt3 - regulation, roles and repercussions for immunotherapy.* Immunol Cell Biol, 2021. **99**(9): p. 962-971.
35. van der Lienden, M.J.C., et al., *Glycoprotein Non-Metastatic Protein B: An Emerging Biomarker for Lysosomal Dysfunction in Macrophages.* Int J Mol Sci, 2018. **20**(1).
36. Gutierrez-Martinez, E., et al., *Cross-Presentation of Cell-Associated Antigens by MHC Class I in Dendritic Cell Subsets.* Front Immunol, 2015. **6**: p. 363.
37. Saftig, P. and R. Puertollano, *How Lysosomes Sense, Integrate, and Cope with Stress.* Trends Biochem Sci, 2021. **46**(2): p. 97-112.
38. Inpanathan, S. and R.J. Botelho, *The Lysosome Signaling Platform: Adapting With the Times.* Front Cell Dev Biol, 2019. **7**: p. 113.
39. Sukhbaatar, N., M. Hengstschlager, and T. Weichhart, *mTOR-Mediated Regulation of Dendritic Cell Differentiation and Function.* Trends Immunol, 2016. **37**(11): p. 778-789.
40. Kaur, S., et al., *Regulatory effects of mammalian target of rapamycin-activated pathways in type I and II interferon signaling.* J Biol Chem, 2007. **282**(3): p. 1757-68.
41. Su, X., et al., *Interferon-gamma regulates cellular metabolism and mRNA translation to potentiate macrophage activation.* Nat Immunol, 2015. **16**(8): p. 838-849.
42. Wang, F., R. Gomez-Sintes, and P. Boya, *Lysosomal membrane permeabilization and cell death.* Traffic, 2018. **19**(12): p. 918-931.
43. Mulder, K., et al., *Cross-tissue single-cell landscape of human monocytes and macrophages in health and disease.* Immunity, 2021. **54**(8): p. 1883-1900 e5.
44. Zhang, H., et al., *Type I interferon remodels lysosome function and modifies intestinal epithelial defense.* Proc Natl Acad Sci U S A, 2020. **117**(47): p. 29862-29871.
45. Ngo, C.C. and S.M. Man, *Mechanisms and functions of guanylate-binding proteins and related interferon-inducible GTPases: Roles in intracellular lysis of pathogens.* Cell Microbiol, 2017. **19**(12).
46. Oliveira, M.M.S. and L.S. Westerberg, *Cytoskeletal regulation of dendritic cells: An intricate balance between migration and presentation for tumor therapy.* J Leukoc Biol, 2020. **108**(4): p. 1051-1065.
47. Bretou, M., et al., *Lysosome signaling controls the migration of dendritic cells.* Sci Immunol, 2017. **2**(16).
48. Nakatani, T., et al., *The lysosomal Ragulator complex plays an essential role in leukocyte trafficking by activating myosin II.* Nat Commun, 2021. **12**(1): p. 3333.
49. Povea-Cabello, S., et al., *Dynamic Reorganization of the Cytoskeleton during Apoptosis: The Two Coffins Hypothesis.* Int J Mol Sci, 2017. **18**(11).
50. Wandel, M.P., et al., *GBPs Inhibit Motility of Shigella flexneri but Are Targeted for Degradation by the Bacterial Ubiquitin Ligase IpaH9.8.* Cell Host Microbe, 2017. **22**(4): p. 507-518 e5.
51. Duong, E., et al., *Type I interferon activates MHC class I-dressed CD11b(+) conventional dendritic cells to promote protective anti-tumor CD8(+) T cell immunity.* Immunity, 2022. **55**(2): p. 308-323 e9.
52. Schaupp, L., et al., *Microbiota-Induced Type I Interferons Instruct a Poised Basal State of Dendritic Cells.* Cell, 2020. **181**(5): p. 1080-1096 e19.